

## Optical nonlinearities due to excitonic molecules: Optical Stark effects and phase conjugation

Eiichi Hanamura

*Department of Applied Physics, University of Tokyo, 7-3-1 Hongo, Bunkyo-ku, Tokyo 113, Japan*

(Received 5 February 1991)

Large, nonlinear-optical phenomena are shown theoretically to be observable under nearly two-photon resonant pumping of the excitonic molecule (EM), e.g., in a CuCl crystal. When the exciton polariton (EP) is resonantly pumped into the EM, they are hybridized with each other and show optical Stark splitting. These splittings can be observed, respectively, as a sharp dip in the reflection spectrum and two-photon absorption spectrum due to the EM. We can also clarify how these splittings change into the blueshifts and redshifts of the EP and the EM as functions of the pump frequency and power. The generation of the phase-conjugated wave is shown also to be enhanced under two-photon resonant pumping of the EM. Some characteristics about pump-probe frequency and polarization dependences are also clarified. We have also derived the effective Hamiltonian of the exciton and the EM from the first-principles equation of motion for the exciton coupled with that of the EM. This Hamiltonian has made possible the theoretical analysis of these nonlinear-optical phenomena.

### I. INTRODUCTION

Since a proposal of giant two-photon absorption due to the excitonic molecule (EM),<sup>1</sup> many enhanced nonlinear-optical phenomena have been observed under two-photon resonant pumping of the EM.<sup>2-9</sup> The EM is a bound state of two single excitons.<sup>10,11</sup> Therefore, two valence electrons must be optically excited to form the EM. The optical transition between the exciton ( $E$ ) and the EM is accompanied with a giant transition dipole moment.<sup>1,12</sup> This comes from the freedom to choose the second valence electron to create the EM inside a large orbital of the EM around the first exciton. Therefore, this originates from the long-ranged Coulomb interaction among two optically excited pairs of electrons and holes, and the itinerant nature of electrons and holes in the conduction and valence bands, respectively. Therefore, this giant transition dipole moment is characteristic of the crystal—the dense and regular arrays of atoms. In this sense, nonlinear-optical phenomena associated with the  $E$  and the EM are very characteristic of the crystal in contrast to those in atomic or molecular systems. As a result, we can expect the enhanced optical nonlinearities under nearly two-photon resonant pumping of the EM. The nonlinear-optical phenomena due to the EM were theoretically described in terms of the three-level model of a crystal ground state, an  $E$  level and an EM level, which was intuitively derived.<sup>13,14</sup> This giant dipole moment and the three-level model of the  $E$  and the EM can be derived in this paper by following an equation of motion derived from first principles for an  $E$  in the crystal coupled with that of an EM. In Sec. II, we derive the equations of motion for an  $E$  and EM from first principles. Then we can discuss under what conditions the effective Hamiltonian is justified. The recent development of laser systems and technologies has made it possible to observe precise spectroscopies in solids. Under such a circumstance we discuss the optical Stark effects

of the  $E$  and the EM under resonant pumping between the exciton polariton (EP) and the EM in Sec. III. In the former works only the optical Stark shift of the exciton was discussed under the off-resonant pumping of the  $E$  (Refs. 15 and 16) or under nearly resonant pumping between the  $E$  and the EM.<sup>17-19</sup> The points of the present paper are as follows: not the  $E$  but the EP is hybridized with the EM by the pump field so that both levels are split and shifted. As a result, we should not simply conclude the blueshift or redshift of the  $E$  but we propose in Sec. III a way to observe these optical Stark effects. The two-photon absorption spectrum due to the EM under the nearly resonant pumping clarifies the splitting of the EM level and the transition to the blueshifts or redshifts of the EM level, depending upon the pump frequency and pump power. This will be shown in Sec. III A. We show also in Sec. III B that the splitting of the EP dispersion under the resonant pumping will be clearly observed as a sharp dip in the reflection spectrum and that this one-photon and two-photon measurement gives us the complementary information on the optical Stark effects. This gives another confirmation of the giant transition dipole moment between the  $E$  and the EM. In Sec. IV, the generation of the phase-conjugated wave is shown to be enhanced under two-photon resonant pumping of the EM. This phase conjugation by the third-order process is discussed in Sec. IV A and this is compared with that due to the polariton-polariton collision process in Sec. IV B. Here we can evaluate the large value of the third-order polarizability  $\chi^{(3)}$  under the nearly two-photon resonant pumping of the EM. We can show that under the resonant pumping of the EM by two pump waves with perpendicular polarizations, the phase conjugation becomes possible by the fifth-order optical processes. This will be discussed in Sec. IV C. Section V is devoted to the discussion and conclusion. Here we will discuss how to distinguish between the coherent distribution of the EM's and the normal states of the EM's by the generation of

the phase-conjugated waves and the future problems on the optical nonlinearity due to the coherent EM's, e.g., on the squeezing through the resonant pumping of the coherent EM's.

## II. EFFECTIVE HAMILTONIAN OF EXCITONS AND EXCITONIC MOLECULES

The crystal is characterized by three-dimensional regular and dense arrays of atoms or molecules. We describe here the electronic system of the crystal in terms of Wannier functions localized at each lattice site, which are made of a linear combination of the Bloch states in the specified conduction band or valence band. The annihilation (creation) operators of the conduction electron in the Wannier-function state localized around the  $j$ th lattice site are denoted by  $c_j$  ( $c_j^\dagger$ ) and the hole operators in the valence-band Wannier state at the  $a$ th site by  $d_a$  ( $d_a^\dagger$ ). We accept a two-band model of the conduction and valence bands. Then the Hamiltonian is given<sup>20</sup> by

$$H = \sum_{i,j} T_{ij}^c c_i^\dagger c_j + \sum_{a,b} T_{ab}^v d_a^\dagger d_b + \frac{1}{2} \sum_{i,j} V_{ij} c_i^\dagger c_i c_j^\dagger c_j + \frac{1}{2} \sum_{a,b} V_{ab} d_a^\dagger d_a d_b^\dagger d_b - \sum_{i,a} V_{ai} c_i^\dagger c_i d_a^\dagger d_a. \quad (2.1)$$

Due to the transfer energies  $T_{ij}^c$  and  $T_{ab}^v$ , electrons and holes can propagate over the whole crystal. These excitations interact with each other by the long-ranged Coulomb interaction  $V_{mn} = \pm e^2 / \epsilon_0 |\mathbf{r}_m - \mathbf{r}_n|$ . Here,  $\epsilon_0$  is a static dielectric constant of the crystal. As a result of combined effects of the excitation transfer and the long-ranged Coulomb interaction, the collective excitations such as an exciton and an excitonic molecule are formed as stable eigenmodes of the excited states of the crystal.

The crystal interacts with radiation field  $E_\lambda$  through the following dipolar interaction:

$$H' = - \sum_{\lambda,j} P_{\lambda j} E_\lambda, \quad (2.2)$$

$$P_{\lambda j} = \mu_{cv} (d_{\lambda j} c_j + c_j^\dagger d_{\lambda j}^\dagger), \quad (2.3)$$

where  $\mu_{cv}$  is a band-to-band transition dipole moment and  $\lambda$  denotes the polarization direction. Here we take a model that the conduction band is made of an  $s$ -state and the valence band of a  $p$ -state the polarization of which is specified by  $\lambda$ .

The exciton state operator  $Y_{ai} \equiv d_a c_i$  obeys the following equation of motion:

$$\begin{aligned} i\hbar \frac{\partial}{\partial t} Y_{ai} &= [H, Y_{ai}] \\ &= H_x^{ai} Y_{ai} + \sum_x (V_{xa} - V_{ix}) (C_{xi} Y_{ax} - D_{xa} Y_{xi}) \\ &\quad - \mu_{cv} (E_a \delta_{ai} - E_a C_{ai} - E_i D_{ai}), \end{aligned} \quad (2.4)$$

where  $a$  denotes both the site and polarization in some cases but only the site in other cases. Here we also introduced two-fermion operators  $C_{ij} \equiv c_i^\dagger c_j$ ,  $D_{ab} \equiv d_a^\dagger d_b$ , and  $Y_{ai}^\dagger \equiv c_i^\dagger d_a^\dagger$ . In the effective-mass approximation, the electron and hole coordinates  $\mathbf{r}_i$  and  $\mathbf{r}_a$  are treated as continuum variables, then a moment expansion is taken for the

transfer-matrix elements  $T_{ij}^c$  and  $T_{ab}^v$ , and we keep only the zeroth-order and isotropic second-order moments. Therefore, the exciton Hamiltonian  $H_x^{ai}$ , which is the first term on the right-hand side of Eq. (2.4), is given in the effective-mass approximation by

$$H_x^{ai} = \hbar\omega_g - \frac{\hbar^2}{2m_e} \nabla_i^2 - \frac{\hbar^2}{2m_h} \nabla_a^2 - \frac{e^2}{\epsilon_0 r_{ai}}, \quad (2.5)$$

where the effective masses  $m_e$  and  $m_h$  are introduced, respectively, at the conduction- and valence-band edges, and  $\hbar\omega_g$  is the band-gap energy.<sup>20</sup> The homogeneous and linear part of Eq. (2.4) is solved, and the eigenenergies and eigenfunctions are given<sup>21</sup> as

$$E_{n\mathbf{K}} \equiv \hbar\omega_n = \hbar\omega_g + \frac{\hbar^2}{2M} K^2 - E_n, \quad (2.6)$$

$$\psi_{n\mathbf{K}} \equiv \psi_n = \frac{1}{\sqrt{V}} e^{i\mathbf{K}\cdot\mathbf{R}} \phi_n(\mathbf{r}). \quad (2.7)$$

The electron-hole relative motion ( $\mathbf{r} \equiv \mathbf{r}_i - \mathbf{r}_a$ ) is described by the hydrogen-like solution  $\phi_n(\mathbf{r})$  and the center-of-mass motion  $\mathbf{R} = (m_e \mathbf{r}_i + m_h \mathbf{r}_a) / M$ , with  $M \equiv m_e + m_h$ , is in the plane-wave state with the wave vector  $\mathbf{K}$ , which is normalized in the crystal volume  $V$ .

As to the higher-order terms in Eq. (2.4), the electron and hole number operators  $C_{xi} \equiv c_x^\dagger c_i$  and  $D_{xa} \equiv d_x^\dagger d_a$  are rewritten in terms of the exciton operators  $Y_{xy}^\dagger$  and  $Y_{yi}$  making use of the relation

$$\sum_y (d_y^\dagger d_y + c_y^\dagger c_y) = 1$$

as follows:<sup>17</sup>

$$\begin{aligned} C_{xi} &\equiv c_x^\dagger c_i \\ &= c_x^\dagger \left[ \sum_y (d_y^\dagger d_y + c_y^\dagger c_y) \right] c_i \\ &= \sum_y (c_x^\dagger d_y^\dagger) (d_y c_i) + O(\hat{Y}^4) \\ &\doteq \sum_y Y_{yx}^\dagger Y_{yi}, \end{aligned} \quad (2.8)$$

$$\begin{aligned} D_{xa} &\equiv d_x^\dagger d_a \\ &= d_x^\dagger \left[ \sum_y (c_y^\dagger c_y + d_y^\dagger d_y) \right] d_a \\ &\doteq \sum_y Y_{xy}^\dagger Y_{ay}. \end{aligned} \quad (2.9)$$

Then the exciton operator  $Y_{ai}$  obeys the following nonlinear equation:

$$\begin{aligned} -i\hbar \dot{Y}_{ai} + H_x^{ai} Y_{ai} \\ + \sum_{xy} (V_{xa} - V_{ix}) (Y_{yx}^\dagger Y_{yi} Y_{ax} - Y_{xy}^\dagger Y_{ay} Y_{xi}) \\ = \mu_{cv} E \left[ \delta_{ai} - \sum_y (Y_{ya}^\dagger Y_{yi} + Y_{iy}^\dagger Y_{ay}) \right]. \end{aligned} \quad (2.10)$$

This is the same expression as that in the boson description of excitons.<sup>22,23</sup> This equation means that the single-exciton motion  $Y_{ai}$  should be solved being coupled

with that of two-exciton  $Y_{ai}Y_{bj} \equiv Z_{ab;ij}$ . Here the suffixes of the  $Z$  operator denote that two holes are located at the lattices  $a$  and  $b$  and two electrons at  $i$  and  $j$ . Note that the radiation field excites the hole in the valence band with the same orbital polarization. The operator  $Z_{ab;ij}$  obeys the following equation:

$$-i\hbar\dot{Z}_{ab;ij} + H_M^{abj}Z_{ab;ij} = \mu_{cv}E(\delta_{ai}Y_{bj} + Y_{ai}\delta_{bj}), \quad (2.11)$$

$$H_M^{abj} = H_x^{ai} + H_x^{bj} + V, \quad (2.12)$$

$$V = V_{ab} + V_{ij} - V_{ai} - V_{bj}. \quad (2.13)$$

Let us consider that the crystal is irradiated by a pump field  $E_p \exp(-i\omega_p t) + c.c$  and a test field  $E_t \exp(-i\omega_t t) + c.c$ . Note, however, that  $E_p \gg E_t$ . Here we may expand the exciton operator  $Y$  and the biexciton operator  $Z$  in terms of their eigenfunctions  $\psi_n$  and  $\Psi_m$ , respectively, as follows:

$$Y_{ai} = \sum_n a_n(t)\psi_n(\mathbf{r}_a, \mathbf{r}_i), \quad (2.14)$$

$$Z_{ab;ij} = \sum_m b_m(t)\Psi_m(\mathbf{r}_a, \mathbf{r}_b; \mathbf{r}_i, \mathbf{r}_j). \quad (2.15)$$

As long as the rotating-wave approximation is accepted, these single-exciton and biexciton states are clearly distinguished. In Eqs. (2.14) and (2.15),  $a_n$  and  $b_m$  are annihilation operators of the  $E$  in state  $|n\rangle$  and the EM in state  $|m\rangle$ . In the lowest order in the external fields,  $a_n(t)$  consists of two frequency components  $a_n(\omega_p)$  and  $a_n(\omega_t)$ , which have time dependences of  $e^{-i\omega_p t}$  and  $e^{-i\omega_t t}$ , and we are interested in the frequency  $(\omega_p + \omega_t)$  component of  $b_m(t)$ , i.e.,  $b_m(\omega_p + \omega_t)$ , which oscillates in  $e^{-i(\omega_p + \omega_t)t}$ . For the orbitally nondegenerate valence and conduction bands such as for CuCl crystal, the molecular bound state of two excitons are possible only for singlet (spin) states both of two electrons and two holes in the excitonic molecule.<sup>10,11,14</sup> We insert these expansions into Eqs. (2.10) and (2.11), multiply  $\psi_n^*(\mathbf{r}_a, \mathbf{r}_i)$  and  $\Psi_m^*(\mathbf{r}_a, \mathbf{r}_b; \mathbf{r}_i, \mathbf{r}_j)$ , re-

spectively, and integrate those over the coordinates. Here we take the expectation values of the radiation fields, the  $E$  and EM operators with respect to the crystal and the radiation system. Then the  $E$  and EM operators as well as the external field can be treated as classical variables. Here and hereafter we use the same notations both for the classical variables and the corresponding operators. Furthermore, we neglect all other terms besides the  $1s$  contribution for a single-exciton state, and linearize with respect to the test field  $E_t$ . Linear response to the pump field alone is obtained from the linear part of Eq. (2.10) as

$$a_{1s}(\omega_p) = \frac{\mu_{cv}\sqrt{V}\phi_{1s}(0)E_p}{\hbar(\omega_{1s} - \omega_p)}, \quad (2.16)$$

where  $\phi_{1s}(0)$  is a value at the origin of the electron-hole relative motion in an exciton and is equal to  $(\pi a_B^3)^{-1/2}$  with exciton Bohr radius  $a_B$ .

The third term on the left-hand side of Eq. (2.10) is written as follows:

$$\begin{aligned} & \sum_{x,y} (V_{xa} - V_{ix})(Y_{yx}^\dagger Y_{yi} Y_{ax} - Y_{xy}^\dagger Y_{ay} Y_{xi}) \\ &= - \sum_{x,y} (V_{xa} - V_{ix})(Y_{yx}^\dagger Z_{ya;xi} - Y_{xy}^\dagger Z_{xa;yi}), \end{aligned} \quad (2.17)$$

$$= \sum_{x,y} Y_{xy}^\dagger (V_{xa} + V_{iy} - V_{ix} - V_{ya}) Z_{xa;yi}. \quad (2.18)$$

Here, Eq. (2.17) is obtained by using the antisymmetric relations  $Z_{ya;ix} \equiv Y_{yi} Y_{ax} = -Z_{ya;xi}$  and  $Z_{ax;yi} \equiv Y_{ay} Y_{xi} = -Z_{xa;yi}$  for exchanges of two electrons or two holes, respectively, with other particles fixed. For derivation of Eq. (2.18), coordinates  $x$  and  $y$  are interchanged in the former half of (2.17). Here we insert the expansions of Eqs. (2.14) and (2.15) into Eq. (2.10), multiply this equation by  $\psi_{1s}^*(\mathbf{r}_a, \mathbf{r}_i)$ , and integrate this over all coordinates. The expectation values are taken both for the  $E$  and EM operators and the radiation field. Then we have the following equation for  $a_{1s}(\omega_t)$ :

$$\begin{aligned} & \hbar(\omega_{1s} - \omega_t)a_{1s}(\omega_t) + \sum_{m,n} W(1s, n; m)a_n^*(\omega_p)b_m(\omega_p + \omega_t) \\ &= \mu_{cv}\sqrt{V}\phi_{1s}(0)E_t - 2\mu_{cv}\sum_{n,n'} \gamma(1s, n; n')a_n^*(\omega_p)[E_p a_n(\omega_t) + E_t a_n(\omega_p)], \end{aligned} \quad (2.19)$$

$$W(1s, n; m) = \sum_{a,i,x,y} \psi_{1s}^*(a, i)\psi_n^*(x, y)V\Psi_m(a, x; i, y), \quad (2.20)$$

$$\gamma(1s, n; n') = \sum_{a,i,x} \psi_{1s}^*(a, i)\psi_n^*(x, y)\psi_n(a, x). \quad (2.21)$$

When the excitonic molecule in the bound state ( $\hbar\omega_b$ ) is almost resonantly pumped by the two-photon ( $\omega_p + \omega_t$ )

transition, we can neglect contributions to the nonlinear-optical responses from the other two-exciton states besides the bound state  $b$  and the other one-exciton state besides the  $1s$  state for the relative motion. This is justified at least for the case of the CuCl crystal, which has a large exciton binding energy of 200 meV and the molecular one 30 meV. Then Eq. (2.17) is simplified as follows. Let us consider the equation of motion for two excitations:

$$i\hbar \frac{\partial}{\partial t} Z_{xa;yi} = (H_x^{ai} + H_x^{xy} + V)Z_{xa;yi} . \quad (2.22)$$

First, we expand  $Z_{xa;yi}$  in terms of eigenstates of two excitations:

$$\begin{aligned} \sum_{x,y,a,i} \psi_{1s}^*(x,y)\psi_{1s}^*(a,i)VZ_{xa;yi} &= \sum_m b_m W(1s, 1; m) \\ &= - \sum_{x,y,a,i} \psi_{1s}^*(x,y)\psi_{1s}^*(a,i)(H_x^{xy} + H_x^{ai} - \hbar\omega_m)\Psi_m b_m \\ &= \sum_m \hbar(\omega_m - 2\omega_{1s})b_m \frac{Q_m}{2\sqrt{V}} , \end{aligned} \quad (2.23)$$

where  $Q_m$  is defined for a bound state of two excitons  $\Psi_b(x, a; y, i)$  as

$$\frac{Q_m}{2\sqrt{V}} \equiv \sum_{x,y,a,i} \psi_{1s}^*(x,y)\psi_{1s}^*(a,i)\Psi_b(x, a; y, i) .$$

Comparing the first and third lines of Eq. (2.23), we have

$$W(1s, 1s; b) = -\hbar(\omega_{1s} - \omega_b/2) \frac{Q_m}{\sqrt{V}} . \quad (2.24)$$

As long as we are confined to the case of the two-photon nearly resonant pumping of the EM, i.e.,  $\omega_b \doteq 2\omega_p$ , only the bound EM state and the  $1s$   $E$  state are responsible for the nonlinear-optical processes. Then inserting the expression Eq. (2.16) of  $a_{1s}^*(\omega_p)$  and the expression of Eq. (2.24) into Eq. (2.19), we have

$$\begin{aligned} \hbar(\omega_{1s} - \omega_t)a_{1s}(\omega_t) - \mu_{cv}\phi_{1s}(0)Q_m E_p^* b(\omega_p + \omega_t) \\ = \mu_{cv}\sqrt{V}\phi_{1s}(0)E_t(1 - \gamma_{SF} - \gamma_{HF}) . \end{aligned} \quad (2.25)$$

Here,

$$\gamma_{SF} = 7 \frac{|\mu_{cv}E_p|^2}{\hbar^2(\omega_{1s} - \omega_p)^2}$$

and

$$\gamma_{HF} = \frac{\Delta_{HF}}{\omega_{1s} - \omega_p} ,$$

where  $\gamma_{SF}$  comes from the state-filling effect and  $\hbar\Delta_{HF}$  is the level shift due to the Hartree-Fock approximation.<sup>17</sup> This shift is an order of 1 meV and the detuning  $\hbar(\omega_{1s} - \omega_p)$  is about 15 meV so that  $\gamma_{SF}$  and  $\gamma_{HF}$  are much less than 1.

Let us derive the equation of motion for  $b(\omega_p + \omega_t)$  from Eq. (2.11). We insert the expansions of  $Y_{ai}$  and  $Z_{ab;ij}$ , i.e., Eqs. (2.14) and (2.15) into Eq. (2.11), multiply this by  $\Psi_b^*(a, b; i, j)$ , and integrate it over the coordinates. Then we have the following equation:

$$\begin{aligned} \hbar(\omega_b - \omega_t - \omega_p)b(\omega_p + \omega_t) - \mu_{cv}\phi_{1s}(0)Q_m^* E_p a_{1s}(\omega_t) \\ = \mu_{cv}\phi_{1s}(0)Q_m^* E_t a_{1s}(\omega_p) . \end{aligned} \quad (2.26)$$

$$Z_{xa;yi} = \sum_m b_m \Psi_m(\mathbf{r}_x, \mathbf{r}_a; \mathbf{r}_y, \mathbf{r}_i) ,$$

multiply  $\psi_{1s}^*(x,y)\psi_{1s}^*(a,i)$  on both sides of Eq. (2.22) and integrate it over the coordinates. Then we have

We have successfully described many nonlinear-optical phenomena due to the excitonic molecule in terms of the following effective Hamiltonian,<sup>6,13,14</sup> which was derived intuitively:

$$\begin{aligned} H_{\text{eff}} &= \sum_{\mathbf{k}} \hbar\omega_{\text{exc}}(\mathbf{k})a_{\mathbf{k}}^\dagger a_{\mathbf{k}} + \sum_{\mathbf{K}} \hbar\omega_m(\mathbf{K})b_{\mathbf{K}}^\dagger b_{\mathbf{K}} \\ &- \sum_{\mathbf{k}} \mu_{\text{exc}}(a_{\mathbf{k}}^\dagger E_{\mathbf{k}} + \text{H.c.}) \\ &- \sum_{\mathbf{K}=\mathbf{k}_1+\mathbf{k}_2} \mu_m(b_{\mathbf{K}}^\dagger a_{\mathbf{k}_0} E_{\mathbf{k}_2} + \text{H.c.}) , \end{aligned} \quad (2.27)$$

where  $\hbar\omega_{\text{exc}}(\mathbf{k}) \equiv E_g + E_{\text{exc}}^b + \hbar^2 k^2/2M$ ,  $\hbar\omega_m(\mathbf{K}) \equiv 2(E_g - E_{\text{exc}}^b) - E_m^b + \hbar^2 K^2/4M$ , and  $\mu_m$  is the giant transition dipole moment between a single  $E$  and an EM.<sup>1,12</sup> Here and hereafter the bound state of the EM will be denoted by a suffix  $m$ . We can justify this effective Hamiltonian by comparing the equations of motion derived from this with Eqs. (2.25) and (2.26) as long as  $\gamma_{SF}, \gamma_{HF} \ll 1$ . At the same time, we can obtain the transition dipole moments  $\mu_{\text{exc}}$  and  $\mu_m$  as

$$\begin{aligned} \mu_{\text{exc}} &= \mu_{cv}\sqrt{V}\phi_{1s}(0) , \\ \mu_m &= \mu_{cv}Q_m\phi_{1s}(0) . \end{aligned}$$

It is noted, however, that the effective Hamiltonian (2.27) is justified only under nearly resonant two-photon pumping of the EM  $2\omega_p \doteq \omega_b$ .

In the case of CuCl crystal, for example, the exciton binding energy  $E_{\text{exc}}^b$  is 200 meV and the molecular binding energy  $E_m^b$  is 30 meV.<sup>9</sup> These come from Coulomb and exchange interactions among electrons and holes, and these interactions have been diagonalized already by introducing the  $1s$   $E$  operator  $a_{\mathbf{k}}$  and the EM operator  $b_{\mathbf{k}}$ . The next largest interaction is the dipolar interaction of the lowest  $1s$  exciton with the radiation field  $E_{\mathbf{k}}$ . This is estimated to be an order of 5 meV from the longitudinal-transverse (LT) splitting.<sup>9</sup> This bilinear interaction is diagonalized into the exciton polariton ( $c_{\mathbf{k}}$  and  $c_{\mathbf{k}}^\dagger$ ) as described by the following equation:

$$\begin{aligned} H_{\text{eff}} &= \sum_{\mathbf{k}} [\hbar\omega_p(\mathbf{k})c_{\mathbf{k}}^\dagger c_{\mathbf{k}} + \hbar\omega_m(\mathbf{k})b_{\mathbf{k}}^\dagger b_{\mathbf{k}}] \\ &+ \sum_{\mathbf{K}=\mathbf{k}_1+\mathbf{k}_2} \hbar g(\mathbf{k}_1, \mathbf{k}_2)b_{\mathbf{K}}^\dagger c_{\mathbf{k}_1} c_{\mathbf{k}_2} + \text{H.c.} \end{aligned} \quad (2.28)$$

Here the coupling constant  $g(\mathbf{k}_1, \mathbf{k}_2)$  between two polaritons and the EM is written in terms of the giant dipole moment  $\mu_m$  and the exciton-to-polariton transformation matrix elements  $C_{11}$  and  $C_{12}$ :<sup>25</sup>

$$\begin{aligned} \hbar g(\mathbf{k}_1, \mathbf{k}_3) &= -\mu_m i \sqrt{(2\pi\hbar\omega_3/V)} C_{11}^*(\mathbf{k}_1) C_{12}^*(\mathbf{k}_3) \\ &\doteq \frac{2\pi\omega_{1s} [\mu_{cv}\phi_{1s}(0)]^2 Q_m}{(\omega_{1s} - \omega_3)\sqrt{V}}. \end{aligned} \quad (2.29)$$

When  $g(\mathbf{k}_1, \mathbf{k}_2)$  is symmetrized with respect to exchange of  $\mathbf{k}_1$  and  $\mathbf{k}_2$ , it should be replaced by

$$\begin{aligned} \frac{1}{2}g_s(\mathbf{k}_1, \mathbf{k}_3) &= -i\frac{\mu_m}{2} \left[ \frac{2\pi}{\hbar V} \right]^{1/2} \\ &\times [\sqrt{\omega_3} C_{11}^*(\mathbf{k}_1) C_{12}^*(\mathbf{k}_3) \\ &\quad + \sqrt{\omega_1} C_{11}^*(\mathbf{k}_3) C_{12}^*(\mathbf{k}_1)]. \end{aligned}$$

As long as  $C_{12}^*(\mathbf{k}_1)$  is neglected as  $ck_1 \gg \omega_{1s}$ , the result is not changed.

Thus we have made it clear under what conditions the effective Hamiltonian Eq. (2.28) is justified.

### III. OPTICAL STARK EFFECT OF THE EXCITONIC MOLECULE

When the pump field  $(\omega_3, \mathbf{k}_3)$  resonantly excites the exciton polariton (EP) at  $\omega_1 = \omega_p(\mathbf{k}_1)$  into the excitonic molecule (EM) at  $\omega_m(\mathbf{k}_2 = \mathbf{k}_1 + \mathbf{k}_3)$ , the EP and the EM are hybridized and strong optical Stark splitting is expected.<sup>26</sup> We will discuss how to observe these splittings by the two-photon absorption spectrum due to the EM in Sec. III A and how to observe these Stark effects on the change of the reflection spectrum in Sec. III B. These two proposals are new in contrast to Refs. 17–19. These optical (or sometimes called dynamical) Stark effects have two characteristics in comparison to the atomic system and the GaAs quantum-well system.<sup>15,16,27,28</sup> First, the present system of the EP and EM shows a stronger splitting by the factor  $Q_m\phi_{1s}(0) \gg 1$ , which comes from the giant transition dipole moment  $\mu_m$  between the  $E$  and the EM. Second, two empty levels of the  $E$  and EM are pumped by the field  $(\omega_3, \mathbf{k}_3)$  so that no real excitations are accompanied.<sup>29,30</sup> Therefore, the rapid switching is expected in this nonlinear-optical process. In the case of CuCl, nobody observed yet two-photon excitations of real electrons and holes under these pumping frequencies. This means that the two-photon absorption process does not become an obstacle against fast switching, as in GaAs quantum wells.

Equations of motion are derived for the annihilation operator of the EP  $c(\mathbf{k}_1) \equiv c_1$  and that of the EM  $b(\mathbf{k}_2) \equiv b_2$  using the effective Hamiltonian Eq. (2.28) and neglecting relaxations of EP and EM as follows:

$$\begin{aligned} i\hbar\dot{c}_1 &= [c_1, H_{\text{eff}}] \\ &= \hbar\omega_p(\mathbf{k}_1)c_1 + \hbar g^*(\mathbf{k}_1, \mathbf{k}_3)c_3^\dagger b_2, \end{aligned} \quad (3.1)$$

$$\begin{aligned} i\hbar\dot{b}_2 &= [b_2, H_{\text{eff}}] \\ &= \hbar\omega_m(\mathbf{k}_2)b_2 + \hbar g(\mathbf{k}_1, \mathbf{k}_3)c_1 c_3. \end{aligned} \quad (3.2)$$

Here,  $c_3 \equiv c(\mathbf{k}_3 = \mathbf{k}_2 - \mathbf{k}_1)\{c_3^\dagger\}$  is an annihilation (creation) operator of the EP with the wave vector  $\mathbf{k}_3 = \mathbf{k}_2 - \mathbf{k}_1$ . Under coherent pumping with the angular frequency  $\omega_3$ , the polaritons  $\omega_p(\mathbf{k}_2 - \mathbf{k}_1) \equiv \omega_3$  are considered to constitute a coherent state:  $c_3|0\rangle_p = A_3 e^{-i\omega_3 t}|0\rangle_p$ . Then the operators  $c_3$  and  $c_3^\dagger$  in Eqs. (3.1) and (3.2) can be replaced by  $A_3 e^{-i\omega_3 t}$  and  $A_3^* e^{i\omega_3 t}$ , respectively. The coupled equations of motion are rewritten as follows:

$$\begin{aligned} [\omega - \omega_p(\mathbf{k}_1)]c_1 - g^*(\mathbf{k}_1, \mathbf{k}_3)A_3^* b_2 e^{i\omega_3 t} &= 0, \\ -g(\mathbf{k}_1, \mathbf{k}_3)A_3 c_1 + [\omega + \omega_3 - \omega_m(\mathbf{k}_2)]b_2 e^{i\omega_3 t} &= 0. \end{aligned}$$

Two eigenfrequencies  $\omega_\pm$  are obtained as

$$\begin{aligned} \omega_\pm &= \omega_1 - \frac{1}{2}(\omega_3 + \omega_1 - \omega_m) \\ &\quad \pm \sqrt{\frac{1}{4}(\omega_3 + \omega_1 - \omega_m)^2 + |gA_3|^2}, \end{aligned} \quad (3.3)$$

where  $\omega_1 \equiv \omega_p(\mathbf{k}_1)$ ,  $\omega_n \equiv \omega_m(\mathbf{k}_2 \equiv \mathbf{k}_1 + \mathbf{k}_3)$ , and  $g \equiv g(\mathbf{k}_1, \mathbf{k}_3)$ . The operators  $b_2$  and  $c_1$  are rewritten in terms of operators  $\alpha_\pm$  corresponding to the eigenfrequencies  $\omega_\pm$  as follows:

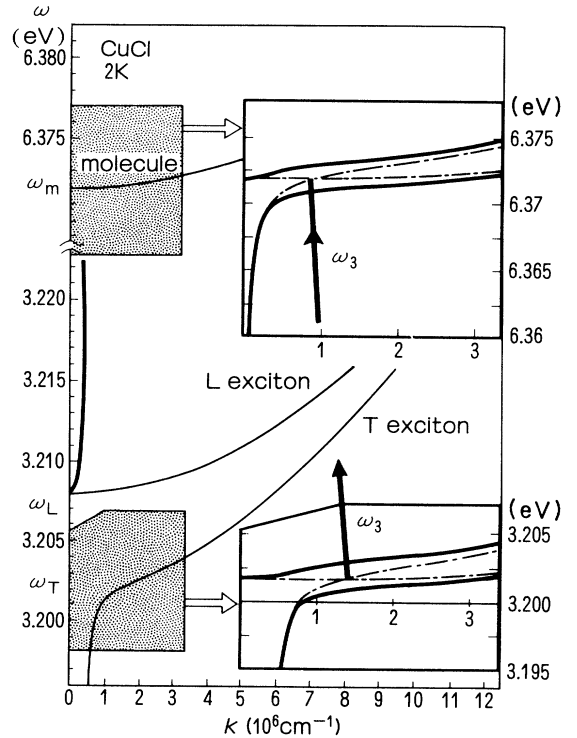


FIG. 1. Dispersion relations of the exciton polaritons (EP) and the excitonic molecule (EM) in the CuCl crystal. The pump field  $\hbar\omega_3 = 3.170$  eV hybridizes the lower-branch EP at  $1.300 \times 10^6 \text{ cm}^{-1}$  with the EM at  $0.888 \times 10^6 \text{ cm}^{-1}$  and induces the splittings of the EM and the EP (---) into the hybridized modes  $\omega_\pm$  (—) as shown in the upper and lower insets.

$$\begin{pmatrix} c_1 \\ b_2 e^{i\omega_3 t} \end{pmatrix} = \begin{pmatrix} C_{a+} & C_{a-} \\ C_{b+} & C_{b-} \end{pmatrix} \begin{pmatrix} \alpha_+ \\ \alpha_- \end{pmatrix}, \quad (3.4)$$

$$C_{a\pm} = \frac{g^* A_3^*}{\sqrt{(\omega_{\pm} - \omega_1)^2 + |g A_3|^2}},$$

$$C_{b\pm} = \frac{\omega_{\pm} - \omega_1}{\sqrt{(\omega_{\pm} - \omega_1)^2 + |g A_3|^2}}.$$

These eigenmodes are hybridized modes of the EP and the EM over the wave vector  $\mathbf{k}_1$  and  $\mathbf{k}_2 = \mathbf{k}_1 + \mathbf{k}_3$  when the pumping EP  $\omega_3 \equiv \omega_p(\mathbf{k}_3)$  pumps the EP  $\omega_1 \equiv \omega_p(\mathbf{k}_1)$  nearly resonantly into the EM  $\omega_m$  ( $\mathbf{k}_2 = \mathbf{k}_1 + \mathbf{k}_3$ ). This is the optical Stark splitting of the EP and the EM as shown in Fig. 1 for  $\hbar|g A_3| = 1$  meV.

The dispersion changes of the EP and the EM due to the pump field  $\omega_3$  will be detected, respectively, by the reflection change around the EP frequency  $\omega_p(\mathbf{k}_1)$  and the giant two-photon absorption due to the EM around  $2\omega_p(\mathbf{k}_0) = \omega_m(\mathbf{k}_2 = 2\mathbf{k}_0)$ . These will be discussed in the following sections.

#### A. Optical Stark splitting detected by two-photon absorption

In this subsection, we evaluate the two-photon absorption spectrum due to the EM under the pumping. The reflection spectrum around  $\omega_0 = \omega_m/2$  is almost constant so that we can well approximate the two-photon absorption spectrum by the conversion rate of two polaritons of  $\omega_p(\mathbf{k}_0)$  into the EM  $\omega_m(2\mathbf{k}_0)$ :

$$\begin{aligned} W^{(2)}[2\omega_p(\mathbf{k}_0)] &= \frac{2}{\hbar} \sum_f \text{Im} \left\langle \mathbf{k}_0 \left| \hbar g^*(\mathbf{k}_0, \mathbf{k}_0) c_{\mathbf{k}_0}^\dagger c_{\mathbf{k}_0}^\dagger b_{2\mathbf{k}_0} \frac{1}{H_f - 2\hbar\omega_p(\mathbf{k}_0) - i\delta} \hbar g(\mathbf{k}_0, \mathbf{k}_0) b_{2\mathbf{k}_0}^\dagger c_{\mathbf{k}_0} c_{\mathbf{k}_0} \right| \mathbf{k}_0 \right\rangle \\ &= 2\pi |g(\mathbf{k}_0, \mathbf{k}_0)|^2 [ |C_{+b}|^2 \delta(\Omega_+ - 2\omega_p(\mathbf{k}_0)) + |C_{-b}|^2 \delta(\Omega_- - 2\omega_p(\mathbf{k}_0)) ], \end{aligned} \quad (3.5)$$

where

$$\begin{aligned} \Omega_{\pm} &= \omega_{\pm} + \omega_3 \\ &= \frac{1}{2} [\omega_p(2\mathbf{k}_0 - \mathbf{k}_3) + \omega_p(\mathbf{k}_3) + \omega_m(2\mathbf{k}_0)] \\ &\quad \pm \left\{ \frac{1}{4} [\omega_p(\mathbf{k}_3) + \omega_p(2\mathbf{k}_0 - \mathbf{k}_3) - \omega_m(2\mathbf{k}_0)]^2 + |g(2\mathbf{k}_0 - \mathbf{k}_3, \mathbf{k}_3) A_3|^2 \right\}^{1/2}. \end{aligned} \quad (3.6)$$

When the pump-polariton  $\mathbf{k}_3$  and the probe-polariton  $\mathbf{k}_0$  propagate in the opposite directions as shown in Fig. 1, the relevant polariton at  $\mathbf{k}_1 = 2\mathbf{k}_0 - \mathbf{k}_3 = 3\mathbf{k}_0$  behaves almost as an exciton so that  $C_{11}^*(\mathbf{k}_1) \doteq 1$ , while the pump polariton at  $\mathbf{k}_3$  behaves almost as a photon, so that<sup>20</sup>

$$C_{12}^*(\mathbf{k}_3) \doteq i\mu_{cv} \phi_{1s}(0) \omega_{1s} \sqrt{2\pi\hbar} / \hbar(\omega_{1s} - \omega_3) \sqrt{V}.$$

Then the splitting at the resonant pumping  $\omega_p(\mathbf{k}_3) + \omega_p(2\mathbf{k}_0 - \mathbf{k}_3) = \omega_m(2\mathbf{k}_0)$ , is estimated from Eq. (2.29) as

$$2|g(\mathbf{k}_1, \mathbf{k}_3) A_3| = \frac{4\pi\omega_{1s} [\mu_{cv} \phi_{1s}(0)]^2 Q_m A_3}{\hbar(\omega_{1s} - \omega_3) \sqrt{V}}. \quad (3.7)$$

For the CuCl crystal and the pump power  $\hbar\omega_3 |A_3|^2 c / (\sqrt{\epsilon_{\infty}} V) = 1$  MW/cm<sup>2</sup>, we can estimate  $\hbar|g(\mathbf{k}_1, \mathbf{k}_3) A_3| = 1$  meV. Here we used the giant oscillator effect  $Q_m^2 = 3600u^3/2$ , where  $u^3 = 40 \text{ \AA}^3$ ,<sup>31</sup> the LT splitting of the EP:  $4\pi\mu_{cv}^2 / (\pi a_B^3 \epsilon_0) = 5.5$  meV and  $\epsilon_{\infty} = 4.66$ .<sup>9</sup> The peak positions  $\Omega_+$  and  $\Omega_-$ , and the relative magnitudes of the oscillator strengths are plotted as a function of the pump frequency  $\omega_3 = \omega_p(\mathbf{k}_3)$  for several values of  $A_3$  in Fig. 2. Note here the following two points. First, the split modes  $\Omega_{\pm}$  are observable with almost the same magnitudes in the frequency detuning  $|\hbar\omega_3 - 3.170 \text{ eV}| \leq \hbar g A_3$ , while under the much larger detuning only one component is observable as the lower part of Fig. 2 shows. Second, the two-photon absorption

due to  $b_2 = C_{b+}\alpha_+ + C_{b-}\alpha_-$  and the linear response due to  $c_1 = C_{a+}\alpha_+ + C_{a-}\alpha_-$  give the complementary information, as will be discussed in the following section. Here the value 3.170 eV is determined as the polariton energy  $\hbar\omega_3 = \hbar\omega_p(\mathbf{k}_3)$ , which satisfies the condition of resonant pumping:  $\omega_p(\mathbf{k}_3) + \omega_p(2\mathbf{k}_0 - \mathbf{k}_3) = \omega_m(2\mathbf{k}_0)$ . Here, two points have been proposed: (1) hybridization of the EP and the EM under resonant pumping between them and (2) observation of the optical Stark splitting by two-photon absorption due to the EM. Gonokami and Shimano<sup>32</sup> observed the optical Stark splitting of the two-photon absorption line due to the EM in good agreement with the present theory. This gives additional support of the giant transition dipole moment between the E and the EM, and the enhanced optical nonlinearity due to the giant transition dipole moment.

#### B. Reflection spectrum

It is shown in this subsection that the hybridization of the EP and the EM can be clearly observed as a sharp dip in the reflection spectrum. Now let us consider a linear response of the EP under the strong pumping. The absorption spectrum of the exciton is broad ( $\sim 5$  meV) due to the transverse-longitudinal splitting of excitons, while the two-photon absorption line due to the EM is sharp ( $\sim 0.02$  meV for the width) and strong due to the giant transition dipole moment. Therefore it is very advanta-

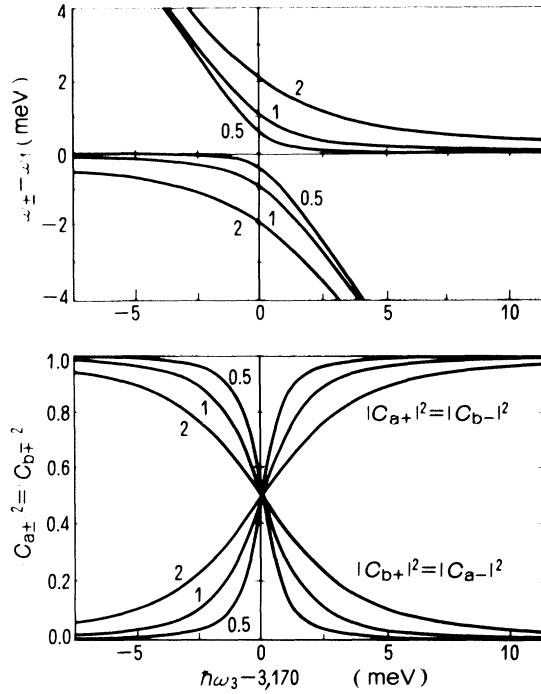


FIG. 2. Upper part: hybridized modes  $\omega_{\pm}$  of the EP  $\omega_p(2\mathbf{k}_0 - \mathbf{k}_3)$  and the EM  $\omega_m(2\mathbf{k}_0)$  as a function of the pump frequency  $\hbar\omega_3 \equiv \hbar\omega_p(\mathbf{k}_3)$ . Note that  $\omega_+ - \omega_1 > 0$  and  $\omega_- - \omega_1 < 0$ . 0.5, 1, and 2 denote, respectively,  $\hbar g(2\mathbf{k}_0 - \mathbf{k}_3)A_3 = 0.5, 1.0,$  and  $2.0$  meV. Lower part: the EP component  $|C_{a\pm}|^2$  and the EM  $|C_{b\pm}|^2$  as a function of  $\hbar\omega_3$ . 0.5, 1, and 2 mean the same as in the upper part.

geous to observe the optical Stark effect by the two-photon absorption spectrum. These Stark effects are, in principle, splittings both of a single-exciton state and a biexciton state (EM). These states, however, are complementary in the following sense. When  $\omega_m(2\mathbf{k}_0) - \omega_p(2\mathbf{k}_0 - \mathbf{k}_3) < \omega_p(\mathbf{k}_3)$ , i.e.,  $\hbar\omega_3 > 3.170$  eV, the redshifted EM ( $C_{b-}$ ) has the larger oscillator strength while the blueshifted EP ( $C_{a+}$ ) has the larger one. For  $\omega_p(\mathbf{k}_3) < \omega_m(2\mathbf{k}_0) - \omega_p(2\mathbf{k}_0 - \mathbf{k}_3)$ , the states with the larger oscillator strength are interchanged both for the EP and the EM states as the lower part of Fig. 2 shows. As a result, we may conclude that the splittings both of the EP and the EM near the resonant pumping  $\omega_m(2\mathbf{k}_0) = \omega_p(\mathbf{k}_3) + \omega_p(2\mathbf{k}_0 - \mathbf{k}_3)$  change into the blueshifts or redshifts of the EP and EM depending upon  $\omega_p(\mathbf{k}_3) \gtrless \omega_m(2\mathbf{k}_0) - \omega_p(2\mathbf{k}_0 - \mathbf{k}_3)$ , when the detuning increases. That is, the EP shifts to the blue side for  $\omega_p(\mathbf{k}_3) \equiv \omega_3 > \omega_m(2\mathbf{k}_0) - \omega_p(2\mathbf{k}_0 - \mathbf{k}_3)$  while it shifts to the red side for  $\omega_3 < \omega_m(2\mathbf{k}_0) - \omega_p(2\mathbf{k}_0 - \mathbf{k}_3)$ . It is, however, rather hard to observe the shift of an order of 1 meV for the broad spectrum with the width 5 meV.<sup>18</sup> It looks advantageous to observe the splitting of the polariton states by the change of the reflection spectrum due to the pump field. Under irradiation of 3.170 eV pump field to excite the polariton at  $k = 1.30 \times 10^6$  cm<sup>-1</sup> into the EM at  $2\mathbf{k}_0 = 8.88 \times 10^5$  cm<sup>-1</sup> in the CuCl crystal, the new mode

of the upper split-off branch appears at 3.202 eV with small wave vector. This mode carries photoenergy so that a sharp dip is marked in the wide-frequency region with high reflectivity due to the LT splitting of the exciton. This phenomenon was already observed in Ref. 4 and analyzed in Refs. 33 and 34. The shape of the reflection dip, however, is sensitive to the wave-number dependence of the polariton relaxation constants. Therefore the one-photon measurement of the optical Stark effect has some disadvantages in comparison to the two-photon measurement. This is a problem for future consideration.

#### IV. PHASE CONJUGATION THROUGH THE EXCITONIC MOLECULE

The forward and backward pump lasers excite the EM at the wave vector  $\mathbf{k} = 0$  coherently by making the best use of giant two-photon absorption process.<sup>1</sup> This process can be also considered as follows: (1) first the forward  $\mathbf{k}_0$  and backward  $-\mathbf{k}_0$  polaritons are excited at the crystal surfaces by the pump lasers, and (2) these polaritons are then converted into the EM at  $\mathbf{k} = 0$ . In the CuCl crystal, this EM has  $\Gamma_1$ -symmetry, and only oppositely circularly polarized components of the two pump polaritons  $\mathbf{k}_0$  and  $-\mathbf{k}_0$  can excite this EM.<sup>35</sup> Therefore when we use the oppositely circularly polarized pump lasers for  $\mathbf{k}_0$  and  $-\mathbf{k}_0$  pump waves, only the EM with  $\mathbf{k} = 0$  can be excited. When we use the linearly polarized pump waves with the parallel polarization, not only the EM's with  $\mathbf{k} = 0$  but also  $\mathbf{k} = 2\mathbf{k}_0$  and  $-2\mathbf{k}_0$  are excited. The probe polariton with wave vector  $\mathbf{k}$  created at the crystal surface by the probe beam stimulates the emission of the polariton with  $-\mathbf{k}$  from the EM at  $\mathbf{k} = 0$  very effectively also using the giant transition dipole moment. This is just the phase-conjugated wave of the probe polariton. The light phase conjugated to the probe light is taken out at the crystal surface. On the other hand, Hasuo *et al.*<sup>36</sup> observed the phase-conjugated wave even under pump-waved  $\mathbf{k}_0$  and  $-\mathbf{k}_0$  with the perpendicular polarizations with the same magnitude as for the case in which the  $\mathbf{k}_0 = 0$  EM can be excited. This question can also be answered in this section in terms of the effective Hamiltonian derived in Sec. II. These processes can also be described by the same effective Hamiltonian Eq. (2.28) as for the optical Stark effects in Sec. III. The generation rate of the phase-conjugated polariton  $\omega_p(-\mathbf{k})$  is evaluated as follows:<sup>37</sup>

$$\begin{aligned} W_{-\mathbf{k}} &= \lim_{t \rightarrow \infty} \frac{d}{dt} \langle t | c_{-\mathbf{k}}^\dagger c_{-\mathbf{k}} | t \rangle \\ &= 2 \lim_{t \rightarrow \infty} \text{Im} \langle 0 | U^\dagger(t) c_{-\mathbf{k}}^\dagger c_{-\mathbf{k}} V U(t) | 0 \rangle \\ &= 2 \text{Im} \langle 0 | T [c_{-\mathbf{k}}^\dagger c_{-\mathbf{k}} V(0) S(\infty, -\infty)] | 0 \rangle. \end{aligned} \quad (4.1)$$

Here the interaction Hamiltonian

$$V = \sum_{\mathbf{K} = \mathbf{k}_1 + \mathbf{k}_2} \hbar g(\mathbf{k}_1, \mathbf{k}_2) b_{\mathbf{K}}^\dagger c_{\mathbf{k}_1} c_{\mathbf{k}_2} + \text{H.c.} \quad (4.2)$$

and

$$S(\infty, -\infty) = \exp \left[ -\frac{i}{\hbar} \int_{-\infty}^{\infty} \tilde{V}(\tau) d\tau \right], \quad (4.3)$$

where  $\tilde{V}(\tau)$  is the interaction representation of  $V$ . The propagator  $U(t) = \exp(-iH_{\text{eff}}t)$  and the initial state  $|0\rangle$  is the coherent states of the EM at  $\mathbf{k}=0$  and the probe polariton  $\omega_p(\mathbf{k})$ .

#### A. Phase conjugation from the $K=0$ excitonic molecule

In this subsection, we rewrite the lowest-order phase-conjugation process in terms of Eq. (4.1) before developing the higher-order processes in Sec. IV C. Let us consider a case where the forward  $\mathbf{k}_0$  and backward  $-\mathbf{k}_0$  pump waves with the opposite circular polarizations excite the EM at  $\mathbf{k}=0$  nearly resonantly. We may assume that both the pump waves and the probe wave as well as the EM at  $\mathbf{k}=0$  constitute the coherent states  $|0\rangle$ :

$$\{c_{\mathbf{k}_0}, c_{-\mathbf{k}_0}, c_{\mathbf{k}} b_0\} |0\rangle = \{A_{\mathbf{k}_0}, A_{-\mathbf{k}_0}, A_{\mathbf{k}}, B_0\} |0\rangle, \quad (4.4)$$

where  $A_{\mathbf{k}_0}$ ,  $A_{-\mathbf{k}_0}$ , and  $A_{\mathbf{k}}$  are the  $c$  numbers and

$$B_0 = \frac{2g(\mathbf{k}_0, -\mathbf{k}_0) A_{\mathbf{k}_0} A_{-\mathbf{k}_0}}{\omega_m(0) - 2\omega_0 - i\gamma_m(0)}. \quad (4.5)$$

Here,  $\omega_0 = \omega_p(\mathbf{k}_0) = \omega_p(-\mathbf{k}_0)$  and  $\gamma_m(0)$  is transverse relaxation rate of the EM at  $\mathbf{k}=0$ . This coherent EM is divided into the probe wave  $\mathbf{k}$  and its phase-conjugated wave  $-\mathbf{k}$ . This process is selectively stimulated by application of the probe beam  $c_{\mathbf{k}}$ . The generation rate of the phase-conjugated wave is evaluated by the lowest-order perturbational expansions as shown diagrammatically in Fig. 3(a):

$$\begin{aligned} W_m^{(3)} &= 2\pi |g(\mathbf{k}, -\mathbf{k}) A_{\mathbf{k}}^* B_0|^2 \delta(\omega_{\mathbf{k}} + \omega_{-\mathbf{k}} - 2\omega_0) \\ &= 8\pi \left| \frac{g(\mathbf{k}_0, -\mathbf{k}_0) g(\mathbf{k}, -\mathbf{k}) (A_{\mathbf{k}_0} A_{-\mathbf{k}_0}) A_{\mathbf{k}}^*}{\omega_m(0) - 2\omega_0 - i\gamma_m(0)} \right|^2 \\ &\quad \times \delta(\omega_{\mathbf{k}} + \omega_{-\mathbf{k}} - 2\omega_0). \end{aligned} \quad (4.6)$$

The same result is obtained for the case that the pump polaritons and the probe polariton do not constitute the coherent state. In this case,  $A_{\mathbf{k}_0}$ ,  $A_{-\mathbf{k}_0}$ , and  $A_{\mathbf{k}}^*$  are replaced by the expectation values of the corresponding polariton operators. This point will be discussed in the final section.

The matrix element  $\hbar g(\mathbf{k}, -\mathbf{k}) A_{\mathbf{k}}^* B_0$  in Eq. (4.6) can be described in terms of the third-order optical susceptibility  $\chi^{(3)}(2\omega_0 - \omega; -\omega_0, \omega, -\omega_0)$ , where the probe wave  $\omega_{\mathbf{k}} = \omega$  and the signal  $\omega_{-\mathbf{k}} = 2\omega_0 - \omega$ . This is done as follows. The third-order polarization corresponding to the generation of the phase-conjugated wave in the cubic crystal like CuCl is written as<sup>38</sup>

$$\begin{aligned} \mathbf{P}^{(3)} &= \alpha(\omega) [(\mathbf{E}_{\mathbf{k}} \cdot \mathbf{E}_{\mathbf{k}_0}) \mathbf{E}_{-\mathbf{k}_0} + (\mathbf{E}_{\mathbf{k}} \cdot \mathbf{E}_{-\mathbf{k}_0}) \mathbf{E}_{\mathbf{k}_0}] \\ &\quad + \beta(\omega) (\mathbf{E}_{\mathbf{k}_0} \cdot \mathbf{E}_{-\mathbf{k}_0}) \mathbf{E}_{\mathbf{k}}. \end{aligned} \quad (4.7)$$

The first two terms describe the generation of phase-conjugated wave due to population gratings made by  $\mathbf{k}$

and  $\mathbf{k}_0$  waves and  $\mathbf{k}$  and  $-\mathbf{k}_0$  waves, and the subsequent reflection of the third wave  $-\mathbf{k}_0$  and  $\mathbf{k}_0$ , respectively. On the other hand, the third term describes the spacially homogeneous process and corresponds to the present mechanism in this section. The last term of Eq. (2.27) is rewritten in terms of the third-order polarization  $\mathbf{P}^{(3)}(\mathbf{K}, \mathbf{k}_1)$  associated with deexcitation of the EM with wave vector  $\mathbf{K}$  into an exciton with  $\mathbf{k}_1$  and the radiation field  $E_{\mathbf{k}_2}$  with  $\mathbf{k}_2 = \mathbf{K} - \mathbf{k}_1$  as

$$\begin{aligned} & - \sum_{\mathbf{k}} \mu_m a_{\mathbf{k}}^\dagger b_0 \cdot \mathbf{E}_{-\mathbf{k}}^* + \text{H.c.} \\ &= - \sum_{\mathbf{k}_1 + \mathbf{k}_2 = 0} \mathbf{P}^{(3)}(0, \mathbf{k}_1) \cdot \mathbf{E}_{\mathbf{k}_2}^* + \text{H.c.} \end{aligned} \quad (4.8)$$

Therefore, the third-order polarization density  $\mathbf{P}^{(3)}(0, \mathbf{k}) \equiv \mu_m a_{\mathbf{k}}^\dagger b_0 / V$  is described in terms of the third-order polarizability  $\beta(\omega) = \chi^{(3)}(2\omega_0 - \omega; -\omega_0, \omega, -\omega_0)$  as follows:

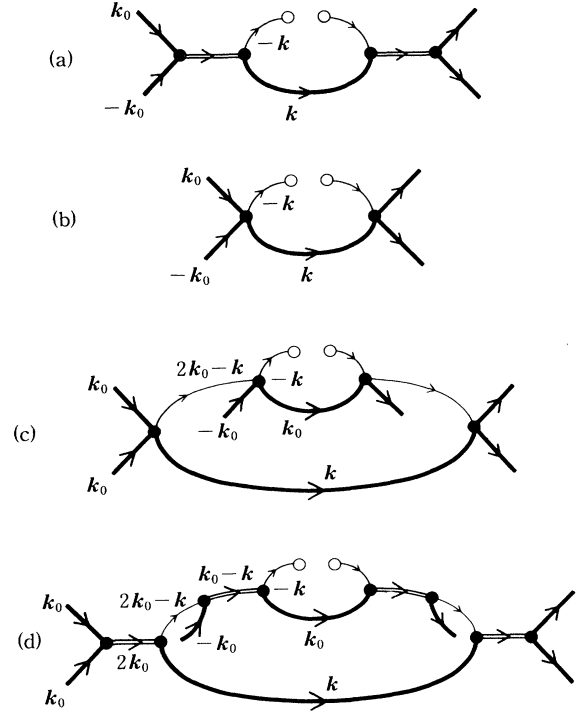


FIG. 3. Feynman diagrams evaluating the generation rate of the phase-conjugated polariton  $-\mathbf{k}$  under the forward  $\mathbf{k}_0$  and backward  $-\mathbf{k}_0$  pump waves and the probe wave  $\mathbf{k}$ ; (a) the third-order processes under nearly two-photon resonant pumping of the EM, (b) third- and (c) fifth-order processes due to the polariton-polariton scatterings, and (d) the fifth-order one due to the EM under the perpendicular polarization  $\mathbf{E}_{\mathbf{k}_0} \perp \mathbf{E}_{-\mathbf{k}_0} \parallel \mathbf{E}_{\mathbf{k}}$ . Solid lines denote the coherent polaritons and double lines denote the propagation of the EM. The thin line denotes the generated single polariton and the circle denotes counting the generation rate of the phase-conjugated polaritons.

$$\begin{aligned} \langle P^{(3)}(0, \mathbf{k}) \rangle &\equiv \mu_m \langle 0 | a_{\mathbf{k}}^\dagger b_0 | 0 \rangle / V \\ &= \beta(\omega) \mathbf{E}_{\mathbf{k}}^* (\mathbf{E}_{\mathbf{k}_0} \cdot \mathbf{E}_{-\mathbf{k}_0}) . \end{aligned} \quad (4.9)$$

Here we consider the probe and the phase-conjugated waves to have the same linear polarization or the opposite circular polarizations. We also assume the coherent states  $\langle 0 | b_0 | 0 \rangle = B_0$  and  $\langle 0 | a_{\mathbf{k}}^\dagger | 0 \rangle = C_{12}^* A_{\mathbf{k}}^*$ . Here the exciton operator  $a_{\mathbf{k}}^\dagger$  at the probe frequency can be approximately rewritten in terms of the lower-branch polariton  $c_{\mathbf{k}}^\dagger$  and the polariton-to-exciton transformation matrix element  $C_{12}^*$ . In the case of CuCl, the probe frequency  $\omega = \omega_p(\mathbf{k})$  is by about 15 meV below the lowest exciton  $\omega_{1s}$  under two-photon resonant pumping of the EM so that  $C_{12}^*$  is approximated by<sup>25</sup>

$$C_{12}^* \doteq i\sqrt{(2\pi\hbar/V)} \mu_{\text{exc}} \omega_{1s} / \hbar(\omega_{1s} - \omega) \sqrt{\omega} . \quad (4.10)$$

The third-order polarizability  $\beta(\omega)$  is evaluated in the present case as

$$\begin{aligned} \beta(\omega) &= \frac{2[\mu_{cv} \phi_{1s}(0)]^4 Q_m^2}{\hbar^3(\omega_{1s} - \omega)(\omega_{1s} - \omega)[\omega_m - 2\omega_0 - i\gamma_m(0)]} \\ &\doteq 10^{-6} i \text{ esu} . \end{aligned} \quad (4.11)$$

Here we assumed the resonant pumping  $2\omega_0 = \omega_m$  and  $\hbar\gamma_m(0) = 0.1$  meV. This extremely large  $\chi^{(3)}$  originates from (1) the resonant enhancement  $\{|2\omega_0 - \omega_m| < \gamma_m(0)\}$  and (2) the giant transition dipole moment  $\mu_{cv} Q_m \phi_{1s}(0)$  ( $\gg \mu_{cv}$ ) between the  $E$  and the EM states. The relaxation rate  $2\gamma_m(0)$  of the EM at  $\mathbf{k} = \mathbf{0}$  is very small at low temperatures in good CuCl crystals. If we have a good sample with  $2\hbar\gamma_m(0) = 0.02$  meV at low temperature,  $\beta(\omega)$  increases to  $10^{-5} i$  esu. Let us summarize several characteristics of the phase conjugation under nearly two-photon resonant pumping of the EM. First, we can expect the extremely large  $\chi^{(3)}$  under nearly two-photon resonant pumping of the EM at  $\mathbf{k} = \mathbf{0}$  by the counterpropagating anticircularly polarized pump waves or linearly polarized pump waves with the parallel polarization. Second, this results in the large phase-conjugated wave, which has the same polarization as the probe wave for the linearly polarized probe wave, but has anticircular polarization for the circularly polarized probe wave. Third, the generation rate shows the peak as a function of the pump frequency  $\omega_0$  when  $2\omega_0 = \omega_m$ . This, however, has a weak dependence on the probe frequency  $\omega$  only through the factor  $(\omega_{1s} - \omega)^{-1}$  in Eq. (4.11), as long as  $\hbar|\omega_{1s} - \omega| \doteq 15$  meV. Fourth, this signal is proportional to  $|A_{\mathbf{k}_0} A_{-\mathbf{k}_0} A_{\mathbf{k}}|^2$ , i.e., linearly proportional to the product of the forward- and backward-pump powers and the probe power.

### B. Phase conjugation due to exciton-exciton collisions

When forward- and backward-pump lights as well as probe light excite only polaritons so that the EM is not resonantly pumped by any two-photon transitions, the exciton-exciton collision and the exciton-impurity

scatterings are responsible for generating of the phase-conjugated signal.<sup>39</sup> These interactions are also rewritten in terms of polariton operators:

$$H'_{\text{pol}} = \frac{1}{2} \sum_{\mathbf{q}, \mathbf{k}_1, \mathbf{k}_2} v(\mathbf{k}_1, \mathbf{k}_2; \mathbf{q}) c_{\mathbf{k}_1 + \mathbf{q}}^\dagger c_{\mathbf{k}_2 - \mathbf{q}}^\dagger c_{\mathbf{k}_2} c_{\mathbf{k}_1} , \quad (4.12)$$

$$H'_{\text{imp}} = \sum_{\mathbf{q}, \mathbf{k}} \sum_i v(\mathbf{q}) e^{i\mathbf{q} \cdot \mathbf{r}_i} c_{\mathbf{k} + \mathbf{q}}^\dagger c_{\mathbf{k}} . \quad (4.13)$$

Here the matrix elements  $v(\mathbf{k}_1, \mathbf{k}_2; \mathbf{q})$  and  $v(\mathbf{q})$  are also obtained by multiplying the exciton-exciton interaction and the exciton-impurity scattering potential, respectively, with products of the exciton-to-polariton transformation matrix elements, as will be shown later. The generation rate of the phase-conjugated wave is given to the lowest order in  $H'_{\text{pol}}$  in Eq. (4.1), which corresponds to the diagram of Fig. 3(b), i.e., the third-order optical process as follows:

$$\begin{aligned} W_{\text{pol}}^{(3)} &= \frac{2\pi}{\hbar^2} [|v_{\text{pol}}(\mathbf{k} + \mathbf{k}_0)|^2 \\ &\quad + |v_{\text{pol}}(\mathbf{k} - \mathbf{k}_0)|^2] |A_{\mathbf{k}_0} A_{-\mathbf{k}_0} A_{\mathbf{k}}^*|^2 \\ &\quad \times \delta(\omega_p(\mathbf{k}) + \omega_p(-\mathbf{k}) - \omega_p(\mathbf{k}_0) - \omega_p(-\mathbf{k}_0)) . \end{aligned} \quad (4.14)$$

Here,  $v(\mathbf{k}_1, \mathbf{k}_2; \mathbf{q})$  is approximated by

$$v_{\text{pol}}(\mathbf{q}) \doteq \frac{26\pi}{3} E_{\text{exc}}^b \frac{a_B^3}{V} C_{12}^*(\omega) C_{12}^*(\omega') C_{12}(\omega_0)^2 , \quad (4.15)$$

when  $\mathbf{k}_1 \doteq \mathbf{k}_2 \doteq \mathbf{0}$  and all four polaritons have the same polarization and spin structures. For two excitons with the same electron spins but perpendicular polarizations,  $v_{\text{pol}}(\mathbf{q})$  becomes half that of Eq. (4.15). This vanishes between two excitons in different spin states. These come from the fact that the exchange process between two excitons is dominant and a simple Coulomb interaction is almost negligible. Here note again that  $\omega_0 = \omega_p(\mathbf{k}_0) = \omega_p(-\mathbf{k}_0)$  for the pump field,  $\omega = \omega_p(\mathbf{k})$  for the probe field, and  $\omega' = 2\omega_0 - \omega = \omega_p(-\mathbf{k})$  for the phase-conjugated signal. We list some characteristics of this four-wave mixing process. First let us compare the relative magnitude of this four-wave mixing with the case of Sec. IV A in which the EM plays the relevant role. The matrix element of these processes is proportional to the third-order susceptibility  $\chi_{\text{pol}}^{(3)}$  as follows:

$$\begin{aligned} \chi_m^{(3)}(2\omega_0 - \omega; -\omega_0, \omega, -\omega_0) &: \chi_{\text{pol}}^{(3)}(2\omega_0 - \omega; -\omega_0, \omega, -\omega_0) \\ &= \hbar g(\mathbf{k}, -\mathbf{k}) A_{\mathbf{k}}^* B_0 : v_{\text{pol}}(\mathbf{k} \pm \mathbf{k}_0) A_{\mathbf{k}}^* A_{\mathbf{k}_0} A_{-\mathbf{k}_0} . \end{aligned} \quad (4.16)$$

Therefore,

$$\begin{aligned} \frac{\chi_{\text{pol}}^{(3)}}{\chi_m^{(3)}} &= \frac{v_{\text{pol}}(\mathbf{k} \pm \mathbf{k}_0) \hbar [\omega_m(0) - 2\omega_0 - i\gamma_m(0)]}{\hbar g(\mathbf{k}, -\mathbf{k}) 2\hbar g(\mathbf{k}_0, -\mathbf{k}_0)} \\ &= -i \frac{26\pi}{3} \frac{a_B^3}{Q_m^2} \frac{E_{\text{exc}}^b \hbar [\omega_m(0) - 2\omega_0 - i\gamma_m(0)]}{\hbar^2(\omega_{1s} - \omega_0)(\omega_{1s} - \omega')} \\ &\doteq -0.1 i , \end{aligned} \quad (4.17)$$

where we used the material constants of CuCl; the exciton Bohr radius  $a_B = 6.7 \text{ \AA}$ ,  $Q_m^2 = 3600 \times u^3 / 2 = 7.2 \times 10^4 \text{ \AA}^3$ ,<sup>28</sup> the exciton binding energy  $E_{\text{exc}}^b = 200 \text{ meV}$ , and  $\hbar\gamma_m(0) = 1 \text{ meV}$ . The value of  $\gamma_m$  depends on the crystal quality and the crystal temperature. The ratio of  $\chi_{\text{pol}}^{(3)}/\chi_m^{(3)}$  will be much reduced for the better crystals with the smaller  $\gamma_m$ . For the present case, we may expect by an order of magnitude (0.02) smaller signal for the present exciton-exciton scatterings in comparison with that of two-photon resonant pumping of the EM. Note here that the present process comes from two channels as Eq. (4.14) shows. Second, the frequency ( $\omega_0, \omega$ ) dependence of this signal intensity is rather weak like  $\omega_0 \sqrt{\omega \omega'} / [(\omega_{1s} - \omega_0)^2 (\omega_{1s} - \omega)(\omega_{1s} - \omega')]$  as long as  $\omega_0, \omega, \omega' \ll \omega_{1s}$ , while the EM process in Sec. IV A shows the peak of the signal intensity at  $2\omega_0 = \omega_m$ . The probe-frequency  $\omega$  dependence relative to the pump-frequency  $\omega_0$  does not show any singularity and any peak for the present process of Fig. 3(b) but the next-higher-order process of Fig. 3(c) shows the peak intensity when  $\omega = \omega_0$ :

$$\begin{aligned} W_{\text{pol}}^{(5)} = & \frac{2\pi}{\hbar^3} \left| \frac{v_{\text{pol}}(\mathbf{k}_0 - \mathbf{k}) v_{\text{pol}}(2\mathbf{k}_0)}{\omega_p(2\mathbf{k}_0 - \mathbf{k}) + \omega_p(\mathbf{k}) - 2\omega_p(\mathbf{k}_0) - i\Gamma} \right|^2 \\ & \times |A_{\mathbf{k}_0}^2 A_{-\mathbf{k}_0} A_{\mathbf{k}}^* A_{\mathbf{k}_0}^*|^2 \\ & \times \delta(\omega_p(\mathbf{k}) + \omega_p(-\mathbf{k}) - \omega_p(\mathbf{k}_0) - \omega_p(-\mathbf{k}_0)). \end{aligned} \quad (4.18)$$

Here,  $\Gamma$  is a sum of the relaxation constants of four polaritons. When the pump-and-probe waves are nearly parallel, the phase-conjugated signal due to the present process shows the peak as a function of the probe-frequency  $\omega$  when  $\omega \equiv \omega_p(\mathbf{k})$  is equal to the pump-frequency  $\omega_0 \equiv \omega_p(\mathbf{k}_0) = \omega_p(-\mathbf{k}_0)$ . The spectrum width is  $2\Gamma$ . This

is the fifth-order optical process and the matrix element of Eq. (4.18) is proportional to  $\chi_{\text{pol}}^{(5)}$ . Let us evaluate the relative magnitude at the peak due to the processes of Figs. 3(b) and 3(c):

$$\begin{aligned} \frac{\chi_{\text{pol}}^{(5)} |E_p|^2}{\chi_{\text{pol}}^{(3)}} = & \frac{v_{\text{pol}}(2\mathbf{k}_0) A_{\mathbf{k}_0} A_{\mathbf{k}_0}^*}{\hbar[\omega_p(2\mathbf{k}_0 - \mathbf{k}) + \omega_p(\mathbf{k}) - 2\omega_p(\mathbf{k}_0) - i\Gamma]} \\ = & i \frac{26\pi E_{\text{exc}}^b a_B^3 A_{\mathbf{k}_0} A_{\mathbf{k}_0}^* (2\pi\hbar\omega_0)^2 \mu_{cv}^4 \phi_{cv}^4(0)}{3\hbar\Gamma V \hbar^4 (\omega_{1s} - \omega_0)^4}. \end{aligned} \quad (4.19)$$

This ratio becomes  $0.2i$  when  $\hbar\Gamma = 1 \text{ meV}$  and the pump power is  $1 \text{ MW/cm}^2$ . Therefore,  $W_{\text{pol}}^{(5)}/W_{\text{pol}}^{(3)} \sim 0.04$  for the present case and the perturbation expansions in the pump powers are justified for the pump power weaker than  $1 \text{ MW/cm}^2$ .

### C. $\chi^{(5)}$ process due to the excitonic molecule

The generation of the phase-conjugated wave under the nearly two-photon resonant pumping of  $\Gamma_1$  EM through the lowest-order process in Fig. 3(a) becomes forbidden when the colliding pump fields  $\mathbf{k}_0$  and  $-\mathbf{k}_0$  have perpendicular linear polarizations. This is easily understood from the fact that this phase-conjugation process is described by  $\beta(\omega)(\mathbf{E}_{\mathbf{k}_0} \cdot \mathbf{E}_{-\mathbf{k}_0}) E_{\mathbf{k}}^*$  and it vanishes when  $\mathbf{E}_{\mathbf{k}_0} \perp \mathbf{E}_{-\mathbf{k}_0}$ . We will show in this subsection that the phase-conjugated wave is induced by the  $\chi^{(5)}$  process described in Fig. 3(d) under this perpendicular configuration  $\mathbf{E}_{\mathbf{k}_0} \perp \mathbf{E}_{-\mathbf{k}_0}$ , and then we will discuss some characteristics of this process. The generation rate due to the  $\chi^{(5)}$  process under pumping with perpendicular polarization is evaluated corresponding to the process in Fig. 3(d) as follows:

$$\begin{aligned} W_m^{(5)} = & 2\pi \left| \frac{g^*(-\mathbf{k}, \mathbf{k}_0) A_{\mathbf{k}_0}^* g(-\mathbf{k}_0, 2\mathbf{k}_0 - \mathbf{k}) A_{-\mathbf{k}_0}}{[\omega_p(-\mathbf{k}) + \omega_p(\mathbf{k}_0) - \omega_m(\mathbf{k}_0 - \mathbf{k}) - i\Gamma']} \frac{g^*(\mathbf{k}, 2\mathbf{k}_0 - \mathbf{k}) A_{\mathbf{k}}^* B_{2\mathbf{k}_0}}{[\omega_p(-\mathbf{k}) + \omega_p(\mathbf{k}_0) - \omega_p(2\mathbf{k}_0 - \mathbf{k}) - \omega_p(-\mathbf{k}_0) - i\Gamma]} \right|^2 \\ & \times \delta(\omega_p(\mathbf{k}) + \omega_p(-\mathbf{k}) - \omega_p(\mathbf{k}_0) - \omega_p(-\mathbf{k}_0)) \quad \text{for } 2\omega_0 \simeq \omega_m \text{ and } \mathbf{E}_{\mathbf{k}_0} \perp \mathbf{E}_{-\mathbf{k}_0} \parallel \mathbf{E}_{\mathbf{k}}. \end{aligned} \quad (4.20)$$

Now let us list some characteristics of this process. First, the phase-conjugated signal has polarization perpendicular to that of the probe wave. Under this configuration, the EM at  $\mathbf{k} = 0$  is not excited and the EM's at  $\mathbf{k} = 2\mathbf{k}_0$  and  $-\mathbf{k}_0$  are induced. The EM's at  $-\mathbf{k}_0$ , however, cannot contribute to the present  $\chi^{(5)}$  process because the  $(-\mathbf{k}_0 - \mathbf{k})$  polariton has polarization perpendicular to the  $\mathbf{k}_0$  polariton so that the EM with  $-\mathbf{k}_0 - \mathbf{k}$  cannot be excited by the polaritons  $\mathbf{k}_0$  and  $-\mathbf{k}_0 - \mathbf{k}$ . Second, the phase-conjugated signal due to this process shows two peaks, as a function of probe frequency  $\omega_0$ , at  $2\omega_0 \equiv 2\omega_p(\mathbf{k}_0) = \omega_m(2\mathbf{k}_0)$  and  $\omega_0 = \omega \equiv \omega_p(\mathbf{k})$  when  $\mathbf{k}$  is nearly parallel to  $\mathbf{k}_0$ . Under nearly two-polariton pumping of the EM or this degenerate four-wave mixing, two denominators should be supplemented with sums of the

relaxation rates of relevant polaritons and/or EM,  $-i\Gamma'$  and  $-i\Gamma$ , respectively. Third, the signal intensity under this configuration is proportional to  $|A_{\mathbf{k}_0}^2 A_{-\mathbf{k}_0} A_{\mathbf{k}}^* A_{\mathbf{k}_0}^*|^2 \equiv I_f^3 I_b I_p$ , which is higher by the factor  $I_f^2 = |A_{\mathbf{k}_0} A_{\mathbf{k}_0}^*|^2$  than that of the  $\chi^{(3)}$  process. This is valid in the case of weak pump-and-probe fields.

Under such a strong pumping as the pump power, which is much larger than  $1 \text{ MW/cm}^2$ , e.g., in CuCl, we must take two effects into account. First, the polaritons at  $\mathbf{k}_0$  and  $-\mathbf{k}_0$  as well as the EM's at  $2\mathbf{k}_0$  and  $-\mathbf{k}_0$  are split by an order of  $|g(\mathbf{k}_0, \mathbf{k}_0) A_{\mathbf{k}_0}|$ , which becomes larger than the detuning  $|\omega_p(\mathbf{k}) - \omega_p(\mathbf{k}_0)|$  and the relaxation constants  $\Gamma'$  and  $\Gamma$ . As a result, roughly speaking, two energy denominators in Eq. (4.20) can be replaced by the

order of the optical Stark shift and cancel out  $g^*(-\mathbf{k}_0, 2\mathbf{k}_0 - \mathbf{k})A_{-\mathbf{k}_0}^*$  and  $g^*(-\mathbf{k}, \mathbf{k}_0)A_{\mathbf{k}_0}$  in the numerator. Then  $W^{(5)}$  becomes of the same order of magnitude and has the same power dependence  $|A_{\mathbf{k}_0}A_{-\mathbf{k}_0}A_{\mathbf{k}}^*|^2$  as the  $\chi^{(3)}$  contribution Eq. (4.6). Second, even under the present polarization, other four-wave mixing due to the  $\chi^{(3)}$  process is possible although the generation of the phase-conjugated wave due to the  $\chi^{(3)}$  process is forbidden. For example, two pump waves with  $\mathbf{k}_0$  ( $-\mathbf{k}_0$ ) excite the EM with  $2\mathbf{k}_0$  ( $-2\mathbf{k}_0$ ) and the probe wave  $\mathbf{k}$  induces the emission of the polariton with  $2\mathbf{k}_0 - \mathbf{k}$  ( $-2\mathbf{k}_0 - \mathbf{k}$ ) when both the energy and wave vector are conserved. This corresponds to the third-order process shown in Fig. 3(a) with the wave vectors modified. These third-order processes attenuate the pump-and-probe waves and these contribute to the relaxation constant  $\Gamma$  and  $\Gamma'$  in Eq. (4.20) as

$$\gamma_{\mathbf{k}} = \pi |g(\mathbf{k}_0, \mathbf{k}_0)B_{2\mathbf{k}_0}A_{\mathbf{k}}^*|^2 \rho(2\mathbf{k}_0 - \mathbf{k}). \quad (4.21)$$

Here,  $\rho(2\mathbf{k}_0 - \mathbf{k})$  is the state density of the polariton at  $2\mathbf{k}_0 - \mathbf{k}$ , which satisfies the energy conservation

$$\omega_p(2\mathbf{k}_0 - \mathbf{k}) = 2\omega_p(\mathbf{k}_0) - \omega_p(\mathbf{k}) \equiv 2\omega_0 - \omega.$$

This energy conservation is nearly satisfied only when the detuning  $|\omega_0 - \omega| \leq \Gamma$  or  $\Gamma'$  for the case that the pump wave  $\mathbf{k}_0$  and the probe wave  $\mathbf{k}$  are closely parallel. Therefore, when such a strong pumping as the  $\chi^{(5)}$  process of Fig. 3(d) becomes of comparable order to the  $\chi^{(3)}$  process of Fig. 3(a), the present four-wave mixing reduces the signal when two conditions  $|\omega_0 - \omega| \leq \Gamma$  or  $\Gamma'$  and  $|2\omega_0 - \omega_m| \leq \Gamma$  or  $\Gamma'$  are satisfied. The latter condition means the enhancement of  $\gamma_{\mathbf{k}}$  through  $|B_{2\mathbf{k}_0}|^2$  in Eq. (4.21). Third, after the EM's at  $2\mathbf{k}_0$  and  $-2\mathbf{k}_0$  are resonantly created, they decay into two polaritons in the order of 50 psec.<sup>28</sup> When the phase-conjugated signals are observed using the laser pulses much longer than 50 psec, the secondary polaritons created by these decay processes enhance the relaxation rate  $\Gamma'$  and  $\Gamma$ .

These characteristics of the  $\chi_m^{(5)}$  process under  $E_{\mathbf{k}_0} \perp E_{-\mathbf{k}_0}$  are consistent with the experimental facts.<sup>36</sup> (a) The phase-conjugated signal under the present process in Sec. IV C is polarized perpendicular to that of the probe wave. (b) The signal is of the same order of magnitude as for the case of the  $\chi_m^{(3)}$  process in Sec. IV A under the off-resonant probe  $\hbar|\omega - \omega_0| \geq 1$  meV when  $|g(\mathbf{k}_0, \mathbf{k}_0)A_{\mathbf{k}_0}| > |\omega - \omega_0|$ , i.e., the pump power is much larger than 1 MW/cm<sup>2</sup> in CuCl. (c) The signals almost vanish for the nearly degenerate case  $\omega = \omega_0$  and  $2\omega_0 = \omega_m$ . This is because the lower-order ( $\chi_m^{(3)}$ ) four-wave mixing inducing the polaritons at  $2\mathbf{k}_0 - \mathbf{k}$  and  $-2\mathbf{k}_0 - \mathbf{k}$  attenuates the pump and signal waves.

## V. DISCUSSION AND CONCLUSION

In Secs. III and IV, we assumed that the EM's that are pumped by the two-photon resonant transition constitute the coherent states. When, however, we integrate the phase-conjugated signal in some frequency width, the

wave signal intensity can be obtained even for normal distributions of the EM's around the relevant  $\mathbf{K}$ . Now let us discuss how to distinguish the coherent EM's, which are Bose condensed in the specified wave-vector state  $\mathbf{K}_0$ , from the normal distribution of EM's. It is possible to create the coherent EM's at the specified wave-vector state  $\mathbf{K}_0$  (Ref. 5) near the origin by pumping, e.g., a CuCl crystal with circularly polarized pump beams  $\mathbf{k}_0$  and  $-\mathbf{k}'_0$  with the opposite rotation and  $\mathbf{K}_0 = \mathbf{k}_0 - \mathbf{k}'_0$ . The coherency of EM's is transferred from the coherent pump beams. This is sometimes called the second kind of Bose condensation. The EM with  $\mathbf{K}_0 = 2\mathbf{k}_0 = 8.88 \times 10^5$  cm<sup>-1</sup> in CuCl relatively decays rapidly, say in 50 psec into two polaritons due to the giant transition dipole moment.<sup>28</sup> Therefore the spectrum width 0.006 meV is inevitable for the EM with  $\mathbf{K}_0 = 8.88 \times 10^5$  cm<sup>-1</sup>. The resonant two-photon transition by a linearly polarized single beam excites the EM at such a wave number  $2\mathbf{k}_0$  as  $\omega_m(2\mathbf{k}_0) = 2\omega_p(\mathbf{k}_0)$ . On the other hand, colliding two beams can excite the EM's at  $\mathbf{K} = 0$  or  $\mathbf{K}$  near the origin. These EM's have a much longer radiative lifetime so that the spectrum broadening is much smaller. This is limited to low lattice temperature and pure crystals in which the EM is not scattered effectively by phonons and imperfections. Under such a circumstance, we will be able to observe the distribution of EM's around the specified  $\mathbf{K}_0$  by the distribution of the phase-conjugated signal due to the  $\chi^{(3)}$  process (Sec. IV A) over  $\omega' = \omega_m(\mathbf{K}) - \omega_p(\mathbf{k})$  and  $\mathbf{k}' = \mathbf{K} - \mathbf{k}$ . When we use the probe beam with high monochromaticity and such a frequency  $\omega$  and wave vector  $\mathbf{k}$  as the signal frequency  $\omega'$  is located in the photon-like branch, a distribution of the EM over the wave-vector state  $\mathbf{K}$  of  $\omega_m(\mathbf{K})$  will be observed with an amplified precision in the frequency region due to the strong dispersion relation. When the probe beam has directionality  $\mathbf{k}$ , the distribution of the EM over  $\mathbf{K}$  will be detected by analyzing the intensity profile of the phase-conjugated signal spot in the radius direction. These observations will be able to distinguish between the coherent or normal distribution of the EM's over the wave-vector state.

The large third-order optical polarizability of an order of  $10^{-5}$  esu, e.g., in good CuCl crystal with  $\hbar\gamma_m = 0.01$  meV, is also characteristic of the  $E$  and the EM system under nearly two-photon resonant pumping of the EM. This results in large optical Stark splittings and a strong generation of the phase-conjugated waves due to the EM's. We can also expect the strong squeezing of the probe and signal lights under the colliding pumpings. This CuCl sample is enough to squeeze the probe and signal under the two-photon resonant pumping of the EM due to the large  $\chi^{(3)}$  value. The degree of the squeezing is also dependent on whether the pumped EM's constitute a coherent state or a normal state. This is also a problem for future consideration.

We have derived in Sec. II the effective Hamiltonian of the  $E$  and the EM from the first-principles equations of motion for excitations in the crystal. This is valid for the description of excitations in I-VII semiconductors such as CuCl and CuBr and II-VI one such as CdS and ZnS in

which the exciton Bohr radius is rather small and the exciton binding energy is large. In III-V semiconductors and IV element semiconductors, we must include the state-filling  $\gamma_{SF}$  and saturation effects  $\gamma_{HF}$ ,<sup>17,24</sup> which were derived in Sec. II. This is because the exciton Bohr radius is very large so that the state-filling effect becomes easily large. The EM is not observed yet in these semiconductors, e.g., in GaAs as the exciton effect is rather small. For the crystals with stable  $E$  and EM such as CuCl, we could describe in terms of this effective Hamiltonian the optical Stark splitting of the EM level and the two-photon absorption measurement of this splitting in Sec. II. At the same time, we could solve how this splitting gradually changes into the redshift and blueshift of the  $E$  level and the EM level as a function of the pump frequency and pump power. This splitting is also shown to be as large as 2 meV when the resonant pumping between the EP and the EM in CuCl is 1 MW/cm<sup>2</sup>. We can also clarify in terms of the Hamiltonian several

characteristics of the strong phase conjugation under resonant two-photon pumping of the EM in Sec. III. Some features of experimental results can be explained in terms of the present theory.

#### ACKNOWLEDGMENTS

The author are grateful to M. Gonokami, A. Mysyrowicz, N. Nagasawa, M. Hasuo, N. Taniguchi, and H. Hiroshima for fruitful discussions and for showing us their results before publication. This work is financially supported by a Grant-in-Aid for Scientific Research on Priority Area, "New Functionality Materials—Design, Preparation, and Control—" and "Electron Wave Interference Effects in Mesoscopic Structures" from the Ministry of Education, Science and Culture of Japan. This was also partially supported by the cooperative research between Japan and France sponsored by Japan Promotion of Sciences.

- <sup>1</sup>E. Hanamura *Solid State Commun.* **12**, 951 (1973).  
<sup>2</sup>G. M. Gale and A. Mysyrowicz, *Phys. Rev. Lett.* **32**, 727 (1974).  
<sup>3</sup>Y. Nozue, T. Itoh, and M. Ueta, *J. Phys. Soc. Jpn.* **44**, 1305 (1978).  
<sup>4</sup>T. Itoh and T. Suzuki, *J. Phys. Soc. Jpn.* **45**, 1939 (1978).  
<sup>5</sup>N. Peyghambarian, L. L. Chase, and A. Mysyrowicz, *Phys. Rev. B* **27**, 2325 (1983).  
<sup>6</sup>G. Mizutani and N. Nagasawa, *J. Phys. Soc. Jpn.* **52**, 2251 (1983).  
<sup>7</sup>M. Kuwata and N. Nagasawa, *Solid State Commun.* **45**, 937 (1983).  
<sup>8</sup>N. Peyghambarian, H. M. Gibbs, M. C. Rushford, and D. A. Weinberger, *Phys. Rev. Lett.* **51**, 1692 (1983).  
<sup>9</sup>For other references on this subject see, e.g., M. Ueta, H. Kanzaki, K. Kobayashi, T. Toyozawa, and E. Hanamura, *Excitonic Processes in Solids* (Springer, Heidelberg, 1986), Chaps. 2 and 3.  
<sup>10</sup>O. Akimoto and E. Hanamura, *J. Phys. Soc. Jpn.* **33**, 1537 (1972).  
<sup>11</sup>W. F. Brinkman, T. M. Rice, and B. Bell, *Phys. Rev. B* **8**, 1570 (1973).  
<sup>12</sup>E. I. Rashba, in *Excitons at High Density*, edited by H. Haken and S. Nikitine (Springer, Heidelberg, 1975), p. 150.  
<sup>13</sup>E. Hanamura, *Solid State Commun.* **38**, 939 (1981).  
<sup>14</sup>H. H. Kranz and H. Haug, *Phys. Rev. A* **34**, 2554 (1986).  
<sup>15</sup>S. Schmitt-Rink, D. S. Chemla, and H. Haug, *Phys. Rev. B* **37**, 941 (1988).  
<sup>16</sup>M. Combescot and R. Combescot, *Phys. Rev. Lett.* **61**, 117 (1988).  
<sup>17</sup>I. Balslev and E. Hanamura, *Solid State Commun.* **72**, 843 (1989).  
<sup>18</sup>D. Hulin and M. Joffre, *Phys. Rev. Lett.* **65**, 3425 (1990).  
<sup>19</sup>M. Combescot (private communication).  
<sup>20</sup>A. Stahl and I. Balslev, *Electrodynamics of the Semiconductor Band Edge* (Springer, Heidelberg, 1987).  
<sup>21</sup>See, e.g., R. S. Knox, in *Theory of Excitons*, edited by F. Seitz and D. Turnbull, *Solid State Physics Suppl.* Vol. 5 (Academic, New York, 1963).  
<sup>22</sup>E. Hanamura *J. Phys. Soc. Jpn.* **29**, 50 (1970).  
<sup>23</sup>E. Hanamura *J. Phys. Soc. Jpn.* **37**, 1545 (1974).  
<sup>24</sup>E. Hanamura and H. Haug, *Phys. Rep.* **30c**, 209 (1977).  
<sup>25</sup>J. J. Hopfield, *Phys. Rev.* **112**, 1555 (1958).  
<sup>26</sup>E. Hanamura, *Solid State Commun.* **77**, 575 (1991).  
<sup>27</sup>A. Mysyrowicz, D. Hulin, A. Antonetti, A. Migus, W. T. Masselink, and H. Morkoç, *Phys. Rev. Lett.* **56**, 2748 (1986).  
<sup>28</sup>A. von Lehmen, D. S. Chemla, J. E. Zucker, and J. P. Heritage, *Opt. Lett.* **11**, 609 (1986).  
<sup>29</sup>D. Fröhlich, A. Nöthe, and K. Reimann, *Phys. Rev. Lett.* **55**, 1335 (1985).  
<sup>30</sup>D. Fröhlich, R. Wille, W. Schlapp, and G. Weimann, *Phys. Rev. Lett.* **59**, 1748 (1987).  
<sup>31</sup>H. Akiyama, T. Kuga, M. Matsuoka, and M. Kuwata-Gonokami, *Phys. Rev. B* **42**, 5621 (1990).  
<sup>32</sup>M. Gonokami and R. Shimano (unpublished).  
<sup>33</sup>R. März, S. Schmitt-Rink, and H. Haug, *Z. Phys.* **40**, 9 (1980).  
<sup>34</sup>V. May, K. Henneberger, and F. Henneberger, *Phys. Status Solidi B* **94**, 611 (1979).  
<sup>35</sup>E. Hanamura, *J. Phys. Soc. Jpn.* **39**, 1506 (1975); **39**, 1516 (1975).  
<sup>36</sup>M. Hasuo *et al.* (unpublished).  
<sup>37</sup>T. Tokihiro and E. Hanamura, *Solid State Commun.* **52**, 771 (1984).  
<sup>38</sup>Y. R. Shen, *The Principles of Nonlinear Optics* (Wiley, New York, 1984), Chap. 14.  
<sup>39</sup>E. Hanamura, *Phys. Rev. B* **39**, 1152 (1989).